Secondary dust density waves excited by nonlinear dust acoustic waves

J. R. Heinrich,[1,a)] S.-H. Kim,[1] J. K. Meyer,[1] R. L. Merlino,[1,b)] and M. Rosenberg[2]
[1]*Department of Physics and Astronomy, University of Iowa, Iowa City, Iowa 52242, USA*
[2]*Department of Electrical and Computer Engineering, University of California, San Diego, California 92093, USA*

(Received 1 May 2012; accepted 24 July 2012; published online 3 August 2012)

Secondary dust density waves were observed in conjunction with high amplitude $(n_d/n_{d0} > 2)$ dust acoustic waves (DAW) that were spontaneously excited in a dc glow discharge dusty plasma in the moderately coupled, $\Gamma \sim 1$, state. The high amplitude dust acoustic waves produced large dust particle oscillations, displacements, and trapping. Secondary dust density waves were excited in the wave troughs of the high amplitude DAWs. The waveforms, amplitudes, wavelengths, and wave speeds of the primary DAWs and the secondary waves were measured. A dust-dust streaming instability is discussed as a possible mechanism for the production of the secondary waves. © *2012 American Institute of Physics*. [http://dx.doi.org/10.1063/1.4742992]

I. INTRODUCTION

It is customary in plasma physics to consider particles and waves as separate entities, realizing that plasma waves involve collective motions of plasma particles which, for electrostatic waves, give rise to propagating coherent oscillations in density and electric fields. The term "particle" in the context of wave-particle interactions actually refers to a small part of the phase space where particle orbits are affected by the resonant interaction between the waves and those particles with speeds near the wave phase speed. For small amplitude plasma waves, particle collisions inhibit nonlinear effects from playing a role; however, when wave amplitudes are sufficiently large, the interactions between waves and particles can become strong, leading to such effects as particle acceleration and trapping. Experimental studies of these nonlinear effects at the microscopic level are generally not possible. Dusty plasmas, which are composed of electrons, ions, neutral atoms, and micron-sized charged particles, afford the capability of studying wave-particle interactions at the microscopic level because the dynamics of the dust can be directly investigated using laser light illumination and fast video imaging techniques.

Dust acoustic waves, which are similar to ion acoustic waves in electron-ion plasmas and sound waves in a gas, are low frequency compressional dust density waves (~tens of Hz), in which the wave inertia is provided by the dust particles.[1] In a glow discharge plasma, dust acoustic waves (DAWs) are spontaneously excited by an ion-dust streaming instability.[2] DAWs can grow to large amplitudes exhibiting non-sinusoidal waveforms[3] or steepen into shocks.[4]

Particle dynamics in high amplitude plasma acoustic waves can result in the creation of sidebands, particle heating, and frequency shifts. For ion-acoustic (IA) waves, Karatzas *et al.*[5] observed sideband and harmonic formation when the waves grew to very large amplitudes $(\tilde{n}_i/n_i \sim 1)$. They attributed these effects to ion trapping in the IA wave troughs and suggested that the trapped ions, acting coherently, might give rise to a two-stream instability.[6] More recently, ion-trapping and the resulting ion heating and frequency shift in saturated ion acoustic waves, driven by simulated Brillion scattering, has been observed by Froula *et al.*[7] These experiments illustrate the importance of particle trapping and displacements by nonlinear IA waves.

Dust particle motion has been measured directly in DAWs.[8] In high amplitude DAWs, dust grains, observed at the particle level, became trapped and traveled with the wavefronts.[9,10] Teng *et al.* observed dust particle displacement, wave breaking, and trapping as DAWs grew to a critical amplitude in a strongly coupled dusty plasma.[10] The wave breaking was later described by Shukla and Lin using a Lagrangian model for strongly coupled dusty plasmas in the presence of an ion flow.[11] In moderately coupled dusty plasmas, DAWs can grow to larger amplitudes without breaking due to weaker inter-particle correlations. These larger amplitude DAWs result in greater particle trapping and displacements and can be used to study wave-particle interactions. Hou and Piel[12] used a Brownian particle simulation to study particle trapping in strongly coupled dusty plasmas (two-dimensional Yukawa liquids). Their numerical results showed that strong coupling effects make it more difficult for trapping to occur while enhancing detrapping. Chang *et al.*[13] experimentally investigated, at the level of individual particle dynamics, the observed absence of trough trapping by self-excited nonlinear dust acoustic waves induced by a downward ion flow in their rf-produced cylindrical dusty plasma. Although the observed washboard type potential wave form compensates the drag force allowing dust with sufficient energy to sustain the oscillatory motion, dust with insufficient energy are trapped in and move with the crest front, preventing them from becoming trapped in the wave trough.

In this paper, we report laboratory observations of spontaneously excited, high amplitude DAWs and associated secondary dust density waves. The large amplitude DAWs $(n_d/n_{d0} > 2$, where n_d is the peak dust density and n_{d0} is the

[a)]Present address: AFRL, Kirtland AFB, New Mexico 87117, USA. Electronic mail: Jonathon.Heinrich.ctr@kirtland.af.mil.
[b)]Electronic mail: robert-merlino@uiowa.edu.

average dust density) displaced a substantial fraction of dust from its equilibrium position, and secondary dust density waves were excited in the restoring drift of the displaced dust particles, possibly due to a dust-dust streaming instability.

II. EXPERIMENTAL SETUP

The experiment was conducted in a dc glow discharge apparatus, 60 cm in diameter and 90 cm in length, shown schematically in Fig. 1. A 300 V bias was applied between the 3.2 cm anode disk and the grounded chamber walls to produce a plasma in argon, at a pressure of 180 mTorr (24 Pa). The ion density, $n_i \sim 2 \times 10^{14}\,\mathrm{m}^{-3}$, and electron temperature, $T_e \approx 2.5\,\mathrm{eV}$, were measured using a double Langmuir probe, while the ion temperature, T_i, was assumed to be $\sim 0.03\,\mathrm{eV}$ [ion Debye length, $\lambda_{Di} = (\varepsilon_o k_B T_i / e^2 n_i)^{1/2} \approx 100\,\mu\mathrm{m}$]. A uniform axial magnetic field of 3 mT was applied to transform the spherical anode glow into an axially elongated firerod.[14] After the plasma was formed, monodisperse, spherical silica dust (radius, $r_d = 0.5\,\mu\mathrm{m}$ and mass, $m_d = 9.4 \times 10^{-16}\,\mathrm{kg}$), located on an electrically insulated tray below the anode, became charged, lifted off the tray, and confined in the firerod,[14] forming a cylindrical dust cloud. The dust density, n_{d0} was $\sim 5 \times 10^{10}\,\mathrm{m}^{-3}$ [interparticle spacing, $\Delta = (3/4\pi n_d)^{1/3} \approx 170\,\mu\mathrm{m}$], while the dust charge, $Q_d = Z_d e$ was estimated using orbital motion limited (OML) theory to be $Q_d \approx -2000e$, where $e = 1.6 \times 10^{-19} C$. The dust in this experiment is most likely in the moderately coupled state, with a Coulomb coupling parameter, $\Gamma = [(Q_d^2/4\pi\varepsilon_o\Delta)/k_B T_d] e^{-\Delta/\lambda_{Di}} \sim 1$.[15]

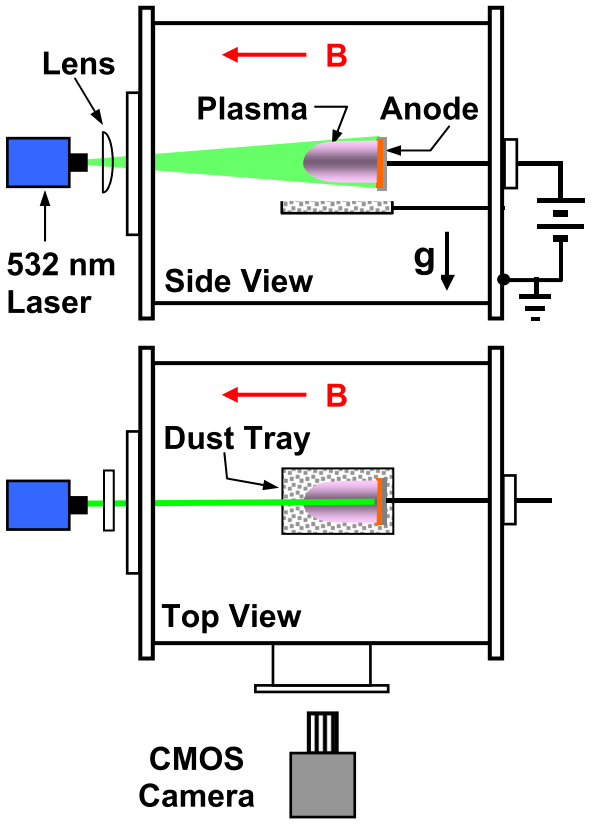

FIG. 1. Schematic of the experimental setup. The plasma is a DC discharge in argon gas at 180 mTorr formed on a 3.2 cm diameter anode disk which is biased at 300 V with respect to the grounded walls of the vacuum vessel (60 cm diam. by 90 cm length). A weak axial magnetic field of 3 mT is applied by a set of 6 external field coils (not shown) to magnetize the electrons and form an axially extended anode glow. Spherical, 1 μm diameter silica dust particles are incorporated into the plasma from a tray located below the anode. The dust particles are illuminated with a narrow vertical sheet of laser light and imaged at 500 frames per second with a CMOS camera.

The primary DAWs were self-excited by ions drifting away from the anode at a speed, $U_{0i} \sim 300\,\mathrm{m/s}$ ($U_{oi}/V_{Ti} \sim 1$, where $V_{Ti} = (k_B T_i/m_i)^{1/2}$ is the ion thermal speed). The ion drift speed was estimated using $U_{0i} = \mu_i E$, where μ_i is the ion mobility[16] and $E \approx 180\,\mathrm{V/m}$ is the axial electric field in the plasma which was measured (in the absence of dust) with an emissive probe.

A sheet of 532 nm laser light illuminated a 2 mm wide vertical slice of the dust cloud, and images of the slice were recorded at 500 frames per second by a Photron (FASTCAM 1024 PCI) CMOS camera at a spatial resolution of 0.06 mm/pixel. The camera has a linear response to light intensity, which allows image intensity to be converted into dust density, n_d, or normalized dust density, $N_d = n_d/n_{d0}$, which were used to characterize the DAWs.

III. OBSERVATIONS AND ANALYSIS

A sample image of the primary DAWs and the secondary dust density waves is shown in Fig. 2(a). The primary DAWs propagated in the direction of the ion flow with an average wave speed ≈36 cm/s, a frequency ≈90 Hz, and a wavelength ≈0.4 cm. The corresponding dust density profile ($N_d = n_d/n_{d0}$), normalized with the time-averaged dust

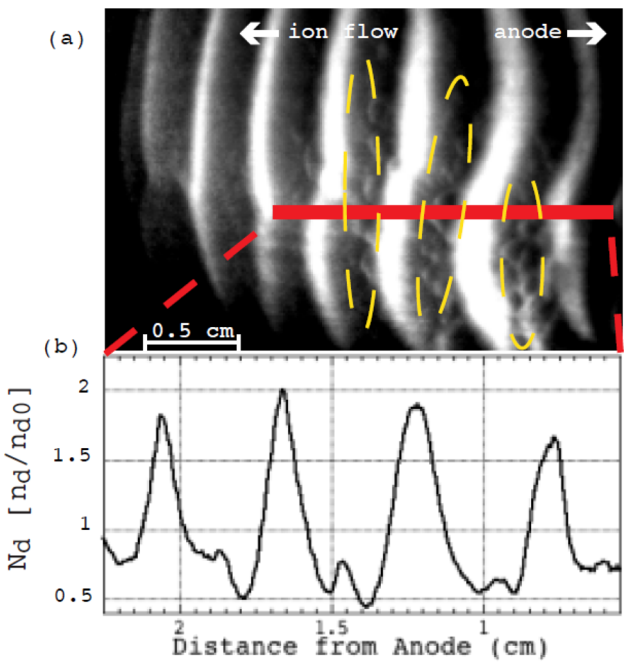

FIG. 2. (a) Single frame video image of the primary and secondary dust density waves. The primary DAWs are the bright vertical wavefronts. The secondary waves (indicated by the dotted yellow ovals) are located in the troughs of the primary waves. (b) The dust density profile taken over the red rectangle, showing the high amplitude primary DAW crests at 0.5 cm, 1.25 cm, 1.65 cm, and 2.15 cm, and the smaller amplitude secondary waves at ~0.95 cm, 1.45 cm, and 1.85 cm from the anode which is to the right side in this figure.

density, n_{d0}, is shown in Fig. 2(b). The secondary mode wavefronts are visible between the brighter wave crests of the primary mode. Typically, the wavefronts of the secondary waves were not uniform across their entire length but were segmented along the direction perpendicular to the direction of propagation.

The primary DAWs were typically of high amplitude as shown in Fig. 2(b). The distribution of primary DAW amplitudes for a sample of 451 wave periods is shown in Fig. 3. The high amplitude (nonlinear) primary DAWs were analyzed by fitting the average wave profile with a wave function containing both first and second harmonic terms,[3,17] assuming that the dust density could be expressed as $n_d = n_{d0} + n_{d1} + n_{d2}$, where n_{d1} and n_{d2} are the first and second order terms in the perturbation expansion, so that the normalized dust density N_d can be written as $N_d = n_d/n_{d0} = 1 + n_{d1}/n_{d0} + n_{d2}/n_{d0}$, with the spatial waveform at an arbitrary time (t = 0)

$$N_d(x,0) = 1 + \tilde{N}_{d1}e^{ikx} + \tilde{N}_{d2}e^{2ikx}, \quad (1)$$

where $\tilde{N}_{d1} = \tilde{n}_{d1}/n_0$ and $\tilde{N}_{d2} = \tilde{n}_{d2}/n_0$ are the normalized amplitudes of the first and second order harmonics. The best fit [Eq. (1)] to the average wave profile was obtained with $N_{d2} = 0.35\ N_{d1}$, is shown in Fig. 4. Figures 3 and 4 indicate that the primary DAWs reached high amplitudes where nonlinear effects were important.

The nonlinear DAWs resulted in dust particle trapping and large amplitude oscillations of the background dust with substantial dust displacements. After each DAW wavefront passed, the background dust (with an average particle displacement of ~0.2 cm, or approximately one-half of a primary wavelength, calculated from the average wave profile) was restored to its equilibrium position with a drift velocity towards the anode.[18] The magnitude of the average (backward) restoring dust drift velocity in the wave trough was estimated at 21 cm/s, or roughly 60% of the phase speed of the primary DAWs. The secondary waves were observed to grow in the drifting dust, and thus were Doppler shifted. A sequence of single-frame video images of the secondary waves and corresponding dust density profiles over a 6 ms interval are shown in Fig. 5. Unlike the nonlinear primary DAWs, the waveforms of the secondary waves were roughly sinusoidal, with nominal amplitudes, $N_{ds} = n_{ds}/n_{d0}$, ranging from 0.65 to 0.75. Compared to the normalized dust density of the wave trough, n_{dt}, these correspond to renormalized wave amplitudes, n_{ds}/n_{dt}, of ~1.1 to 1.5, with a nominal value of ~1.25. The secondary waves propagated (in the lab frame) towards the anode, but at a much slower velocity than the drifting dust, indicating the secondary waves were compressional waves. Often, multiple secondary waves were excited in a single primary wave trough, as shown in Fig. 5. For these cases, the secondary waves had an average wavelength of 0.12 ± 0.02 cm. The average laboratory phase speed of the secondary waves was 10 ± 5 cm/s, towards the anode. The measured wavelength and wave speed of the secondary waves gives a frequency of ~80 Hz. The parameters of the primary DAWs and the secondary dust density waves are summarized in Table I.

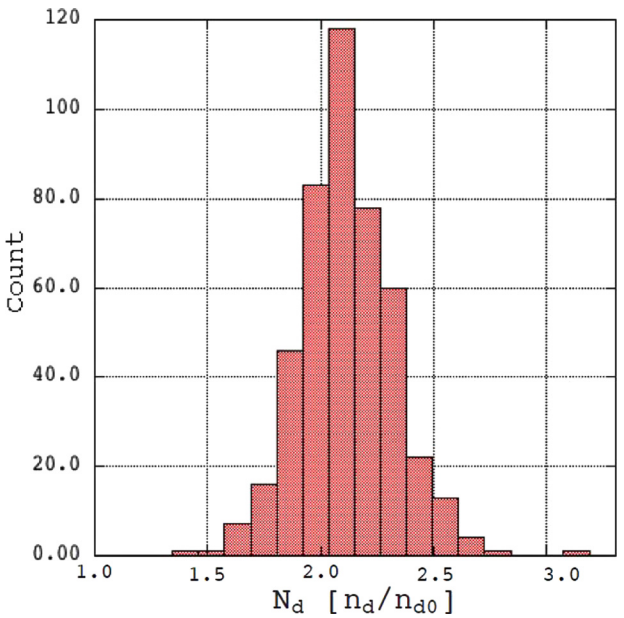

FIG. 3. The distribution of the amplitudes of 451 primary dust acoustic waves. While wave amplitudes $N_d \sim 1$ are common, wave amplitudes over 2 were sometimes observed.

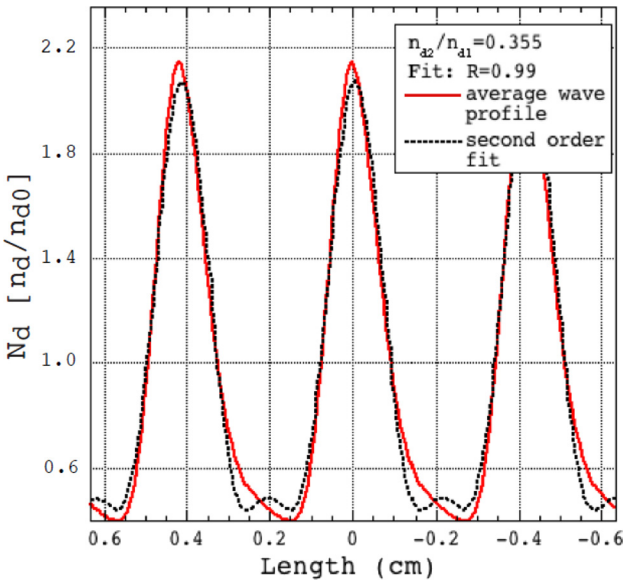

FIG. 4. Averaged primary wave profile taken over 300 waves. The average wave profile (shown in red) was fit (dashed line) with a wave function [Eq. (1)] which included both first and second harmonic terms.

IV. DISCUSSION

Since the secondary waves occur when a fraction of the dust grains have a drift velocity towards the anode, an intriguing possible mechanism for the excitation of these waves propagating towards the anode is a dust-dust streaming instability.[19] The dust-dust instability is the low frequency analog of the ion-ion instability.[20] To very roughly estimate the conditions for growth of the dust-dust instability we consider the following simple model. The dusty plasma is composed of ions, electrons, neutral atoms, and two species of dust grains. The ions have a drift away from the

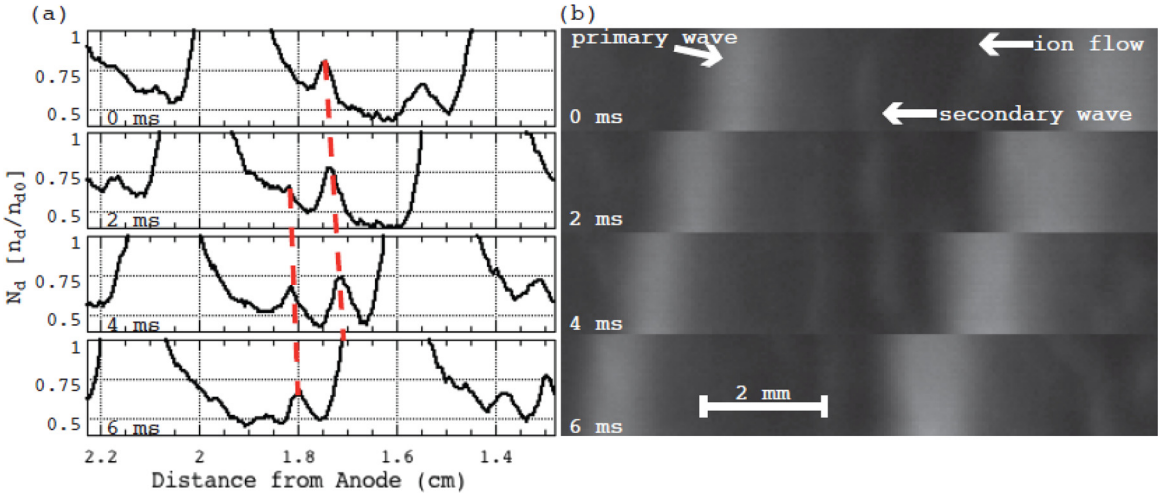

FIG. 5. Right side: sequence of single frame video images of primary and secondary dust density waves at 0 ms, 2 ms, 4 ms, and 6 ms, showing that the primary waves travel away from the anode while the secondary waves travel toward the anode. Left side: corresponding dust density profiles obtained from the images. The red dotted lines show the progression in time of the secondary waves. In this case, two secondary waves are excited in the primary wave trough.

anode (taken as the "+" direction), and the electrons and one of the dust species have a drift toward the anode (the "–" direction), while the other dust species is stationary. It is assumed that the velocity distributions can be modeled by Maxwellians or drifting Maxwellians as appropriate. Collisions of charged particles with neutrals are taken into account. Under these assumptions, the following one-dimensional kinetic dispersion relation can be used to model the dust-dust instability:

$$1 + \chi_e + \chi_i + \chi_{d1} + \chi_{d2} = 0, \tag{2}$$

where the subscripts $\alpha = e$, i, $d1$, and $d2$ refer to electrons, ions, dust species 1 and 2, respectively, and where

$$\chi_\alpha = \frac{\sqrt{2}kV_{T\alpha} + (\bar{\omega} + i\nu_{\alpha n})Z(\zeta_\alpha)}{k^2\lambda_{D\alpha}^2[\sqrt{2}kV_{T\alpha} + i\nu_{\alpha n}Z(\zeta_\alpha)]}, \tag{3}$$

with $\bar{\omega} = \omega + kU_{0\alpha}$ and $\zeta_\alpha = (\bar{\omega} + i\nu_{\alpha n})/\sqrt{2}kV_{T\alpha}$. Here $\lambda_{D\alpha} = (\varepsilon_o k_B T_\alpha/n_\alpha e^2)^{1/2}$, $\nu_{\alpha n}$ is the neutral-charged particle collision frequency, $V_{T\alpha} = (k_B T_\alpha/m_\alpha)^{1/2}$ is the thermal speed, m_α is the mass of species α, and $U_{0\alpha}$ is the drift speed of species α, which is negative in the direction toward the anode.

The dispersion relation (2) was solved numerically, using parameters representative of the experimental conditions, and dust densities $n_{d1} \sim n_{d2} \sim 2.5 \times 10^{10}\,\mathrm{m}^{-3}$. The collision rates of electrons and ions with neutrals were estimated using $\nu_{jn} \sim N\sigma_{jn}V_{Tj}$ for $j = e$, i (with the cross sections for electron-neutral and ion-neutral collisions, respectively, $\sigma_{en} \sim 5 \times 10^{-20}$ m^2 and $\sigma_{in} \sim 5 \times 10^{-19}$ m^2), where N is the neutral atom density. The dust-neutrals collision rate[21] is given by $\nu_{dn} \sim (8\sqrt{2\pi}/3)r_d^2 N V_{Tn} m_n/m_d$, where V_{Tn}, m_n, and m_d are the neutral thermal speed, neutral mass, and dust mass, respectively. The resulting ion Debye length, $\lambda_{Di} \sim 0.1$ mm, and the dust plasma frequency associated with each dust species is, $\omega_{pd1} \sim \omega_{pd2} \sim 556\,\mathrm{s}^{-1}$. The dust thermal (kinetic) energy is not known, but we take it to be about $T_d \sim T_e \sim 2.5$ eV. For the particle drifts, we take $U_{0i}/V_{Ti} = +1.5$, $U_{0e}/V_{Te} = -0.2$, and $U_{0d}/V_{Td} = -8$ (corresponding to $|U_{0d}| \sim 17$ cm/s). The real ω_r and imaginary γ parts of the frequency versus $k\lambda_{Di}$ obtained by solving the dispersion relation are shown in Fig. 6. It appears that linear growth is possible under these conditions, with a maximum growth rate γ_{max} of about $154\,\mathrm{s}^{-1}$ at $k\lambda_{Di} \sim 0.6$ (wavelength ~ 1 mm). In addition, the phase speed of the unstable dust wave is about $U_{0d2}/2$, as would be expected on the basis of ion-ion instability for a symmetric (i.e., $\omega_{pd1} = \omega_{pd2}$) case.[20]

TABLE I. Parameters of primary dust acoustic waves and secondary dust density waves.

Parameter	Primary DAW	Secondary wave
Wavelength (cm)	0.4 ± 0.04	0.12 ± 0.04
Wave speed (cm/s)	36 ± 4	−10 ± 5
Frequency (Hz)	90 ± 13	80 ± 50 (lab frame)
Normalized amplitude	2.2	0.65 to 0.75

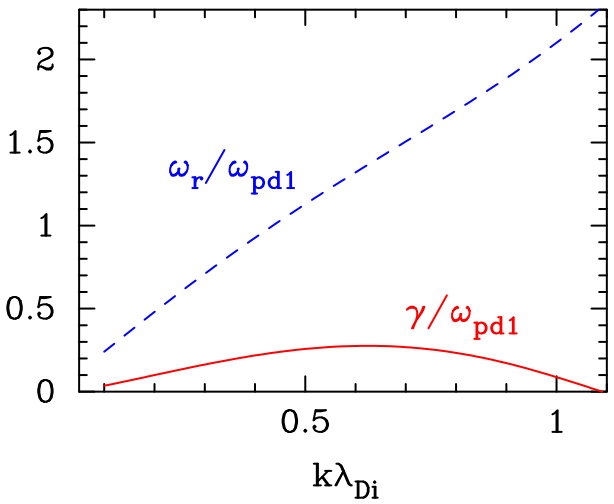

FIG. 6. Real and imaginary parts of ω normalized to ω_{pd1} versus the wavenumber $k\lambda_{Di}$ obtained by solving numerically the dispersion relation [Eq. (2)] for the dust-dust streaming instability. Parameters used were $T_e/T_i = T_d/T_i = 83$, $m_d/m_p = 5.64 \times 10^{11}$, $Z_d = Q_d/e = 2000$, $n_{d1}/n_i = n_{d2}/n_i = 1.25 \times 10^{-4}$, $\nu_{en}/\omega_{pi} = 67$, $\nu_{dn}/\omega_{pi} = 6 \times 10^{-5}$, $\nu_{in}/\omega_{pi} = 0.28$, $U_{0i}/V_{Ti} = 1.5$, $U_{0e}/V_{Te} = -0.2$, and $U_{0d}/V_{Td} = -8$.

Although the results appear to be reasonably consistent with the observations as regards the wavelength and phase speed of the secondary waves, we need to point out a number of caveats regarding both the applicability and assumptions of this model. First, the moving dust species streams toward the anode for a time on the order of only twice the growth time of the instability. For example, assuming the dust moves a displacement distance of about 0.2 cm, and its speed is about 17 cm/s, then it streams for only about 12 ms, which is about twice $\gamma_{\max}^{-1}$ estimated above. Thus, it appears that the wave amplitude could grow by a factor of about $e^2 \sim 7$ out of the thermal noise. It is not clear if this is sufficient to be observed. Second, the assumption of Maxwellian or drifting Maxwellian velocity distributions may not be appropriate since the large amplitude primary wave can lead to trapping of the ions and/or the dust which can distort the distributions. Third, although it was assumed the dust is in the gaseous phase, the bare dust Coulomb coupling parameter, $\Gamma_C = [(Q_d^2/4\pi\varepsilon_o\Delta)/k_B T_d]$, where Δ is the average intergrain spacing, is about 10 for each dust species for the assumed parameters. If we assume a plasma screening length $\lambda_D \sim \lambda_{Di}$, the screened Coulomb coupling parameter $\Gamma_C e^{-\Delta/\lambda_D} \sim 1$, so the dust is marginally in the gaseous phase and weakly coupled theory may roughly apply. However, if the plasma screening length is $\lambda_{De} \sim 0.1$cm, the screened Coulomb coupling parameter is on the order of 10 and strong coupling effects could modify the results somewhat.

V. CONCLUSION

In a dc-discharge dusty plasma device, high amplitude, self-excited nonlinear DAWs were observed to produce large oscillations and displacements in the background dust. The high amplitude DAWs were characterized using second order wave theory. In the troughs of the high amplitude DA waves secondary dust density wave were observed, which propagated in the direction *opposite* to that of the primary waves. The secondary dust density waves were characterized by their waveform, phase velocity, and wavelength.

A possible mechanism for the excitation of the secondary dust waves is a dust-dust streaming instability due to the restoring drift of the dust. A simple model for this instability was presented, and the numerical results indicated that this could provide a mechanism for the growth of the secondary waves.

ACKNOWLEDGMENTS

We thank M. Miller for technical assistance. The work at UI was supported by DOE Grant DE-FG01-04ER54795 and NSF Grant PHY-0923141. The work at UCSD was supported by NSF Grant PHY-0903808 and NASA Grant NNX10AR54G.

[1]N. N. Rao, P. K. Shukla, and M. Y. Yu, Planet. Space Sci. **38**, 543 (1990).
[2]See, e.g., R. L. Merlino, Phys. Plasmas **16**, 124501 (2009) and references therein.
[3]R. L. Merlino, J. Heinrich, S.-H. Kim, and J. K. Meyer, Phys. Plasmas **19**, 057301 (2012).
[4]B. Eliasson and P. K. Shukla, Phys. Rev. E **69**, 067401 (2004); J. Heinrich, S.-H. Kim, and R. L. Merlino, Phys. Rev. Lett. **103**, 115002 (2009).
[5]N. T. Karatzas, A. J. Anastassiadis, and K. Papadopoulos, Phys. Rev. Lett. **35**, 33 (1975).
[6]A simple model for a two-stream instability driven by particles trapped in large-amplitude electrostatic waves was presented by W. L. Kruer, J. M. Dawson, and R. N. Sudan, Phys. Rev. Lett. **23**, 838 (1969).
[7]D. H. Froula, L. Divol, A. A. Offenberger, N. Meezan, T. Ao, G. Gregori, C. Niemann, D. Price, C. A. Smith, and S. H. Glenzer, Phys. Rev. Lett. **93**, 035001 (2004).
[8]E. Thomas and R. Merlino, IEEE Trans. Plasma Sci. **29**, 152 (2001); C.-T. Liao, L.-W. Teng, C.-Y. Tsai, C.-W. Io, and I. Lin, Phys. Rev. Lett. **100**, 185004 (2008).
[9]M. Schwabe, M. Rubin-Zuzic, S. Zhdanov, H. M. Thomas, and G. E. Morfill, Phys. Rev. Lett. **99**, 095002 (2007).
[10]L.-W. Teng, M.-C. Chang, Y.-P. Tseng, and I. Lin, Phys. Rev. Lett. **103**, 245005 (2009).
[11]P. Shukla and I. Lin, Phys. Lett. A **374**, 1165 (2010).
[12]L.-J. Hou and A. Piel, Phys. Plasmas **15**, 073707 (2008).
[13]M.-C. Chang, L.-W. Teng, and I. Lin, Phys. Rev. E **85**, 046410 (2012).
[14]T. An, R. L. Merlino, and N. D'Angelo, J. Phys. D **27**, 1906 (1994); T. Trottenberg, D. Block, and A. Piel, Phys. Plasmas **13**, 042105 (2006).
[15]The coupling parameter Γ was estimated assuming a dust temperature $T_d \sim T_e$. The dust temperature was not measured in this experiment, but other investigators who used similar devices [see, J. D. Williams, E. Thomas, Jr., and L. Marcus, Phys. Plasmas **15**, 043704 (2008); E. Thomas, Jr., Phys. Plasmas **17**, 043701 (2010)] measured dust temperatures much higher than the electron temperature, probably due to dust heating by the DAWs. If $T_d \gg T_e$ in our experiments, then $\Gamma \ll 1$, and the dust would have been in the gaseous state.
[16]S. Robertson and Z. Sternovsky, Phys. Rev. E **67**, 046405 (2003).
[17]R. L. Merlino, Phys. Scr. **85**, 035506 (2012).
[18]Similar measurements were reported in Ref. 10.
[19]A fluid theory for instability of counterstreaming cold dust beams was given by P. K. Shukla and N. N. Rao, Phys. Scr. **T75**, 288–289 (1998).
[20]T. Fujita, T. Ohnuma, and S. Adachi, Plasma Phys. **19**, 875 (1977).
[21]P. K. Shukla and A. A. Mamun, *Introduction to Dusty Plasma Physics* (IoP, Bristol, 2002), p. 79.